# Supplementary Information

## Highly sensitive biosensor with resonant coupling of plasmon-waveguide resonance to localized surface plasmons

Huimin Wang[a,1], Enze Lv[a,1], Tao Wang[a,*], Xinzhao Yue[a], Jinwei Zeng[a], Wenyu Zhao[a,*], and Jian Wang[a,*]

[a] Wuhan National Laboratory for Optoelectronics, Huazhong University of Science and Technology, Wuhan, 430074, China.

[1] Huimin Wang and Enze Lv contributed equally to this work.

* Corresponding author: Email: wangtao@hust.edu.cn; zhaowenyu@hust.edu.cn; jwang@hust.edu.cn

**S1.** Materials

Primary antibody of CEA ($Ab_1$), CEA, and secondary antibody of CEA ($Ab_2$) were from Beijing Key-Bio Biotech Co.Ltd (Beijing, China). Phosphate-buffered saline (PBS), bovine serum albumin (BSA), 11-mercaptoundecanoic acid (MUA), N-hydroxysuccinimide (NHS), and N-(3-Dimethylaminopropyl)-N′-ethylcarbodiimide hydrochloride (EDC) were from Sigma-Aldrich (Shanghai, China). Mouse serum was purchased from Shanghai yuanye Bio-Technology Co., Ltd (Shanghai, China). Tannic acid, sodium citrate, $KCO_3$, 4-morpholineethanesulfonic acid (MES), and HS-PEG-COOH were from Shanghai Macklin Biochemical Co., Ltd. (Shanghai, China).

***S2. Preparations of the AuNPs and AuNP-$Ab_2$***

***2.5 mM tannic acid (0.5 μL), 2.2 mM sodium citrate (75 mL), and 150 mM $KCO_3$ (0.5 mL) were mixed together, and then heated to 100 °C. 25 mM $HAuCl_4$ solution (0.5 mL) was subsequently added. The reaction was carried out at 100 °C for 20 minutes until the solution turned orange-red, indicating that AuNPs were successfully prepared.***

***AuNPs were combined with HS-PEG-COOH by gently stirring for 10 h to obtain the carboxyl modified AuNP (AuNP-COOH). The AuNP-COOH solution was centrifuged twice, and then the AuNP-COOH was dispersed in the MES solution (pH***

*5.5). After the carboxyl group of the AuNP-COOH was activated by a mixture of EDC and NHS, the resulting solution was centrifuged once. The activated AuNP-COOH reacted with 25 μg/mL $Ab_2$ for 10 h, and the product was then dispersed in PBS with 0.1% BSA solution to obtain the AuNP-$Ab_2$ solution. The resulting solution was centrifuged twice. The AuNP-$Ab_2$ was then dispersed in PBS, and the preparation of the AuNP-$Ab_2$ was complete. The centrifugation time and centrifugal rate for each cycle were 30 min and 13000 rpm, respectively.*

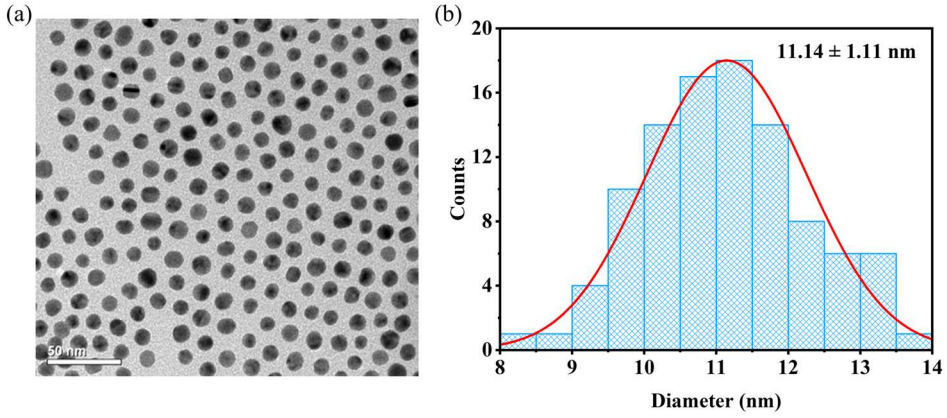


*Fig. S1 TEM image (a) and diameter distribution diagram (b) of AuNPs.*

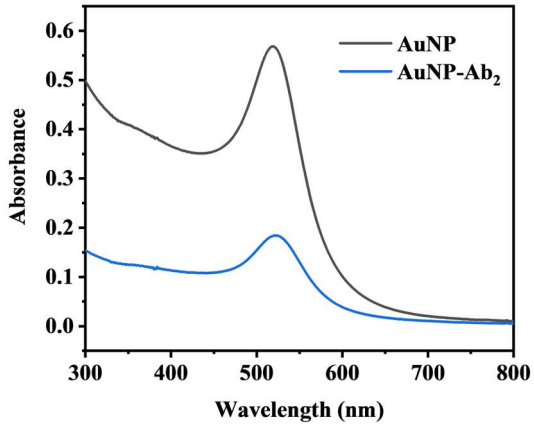


*Fig. S2 UV-VIS absorption spectra of AuNPs and AuNP-$Ab_2$ solutions.*

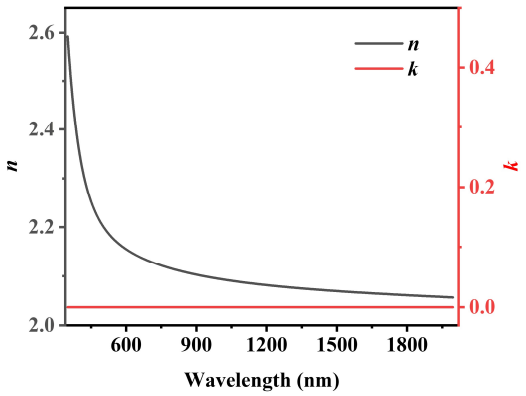


**Fig. S3** Refractive index characterization of $TiO_2$.

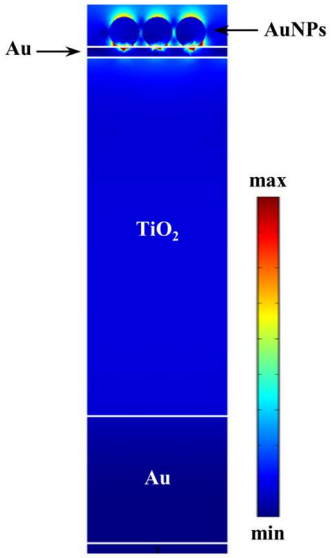


***Fig. S4 Electric field distribution of the Au-$TiO_2$-AuNPs structure within a 4 nm Au functional layer.***

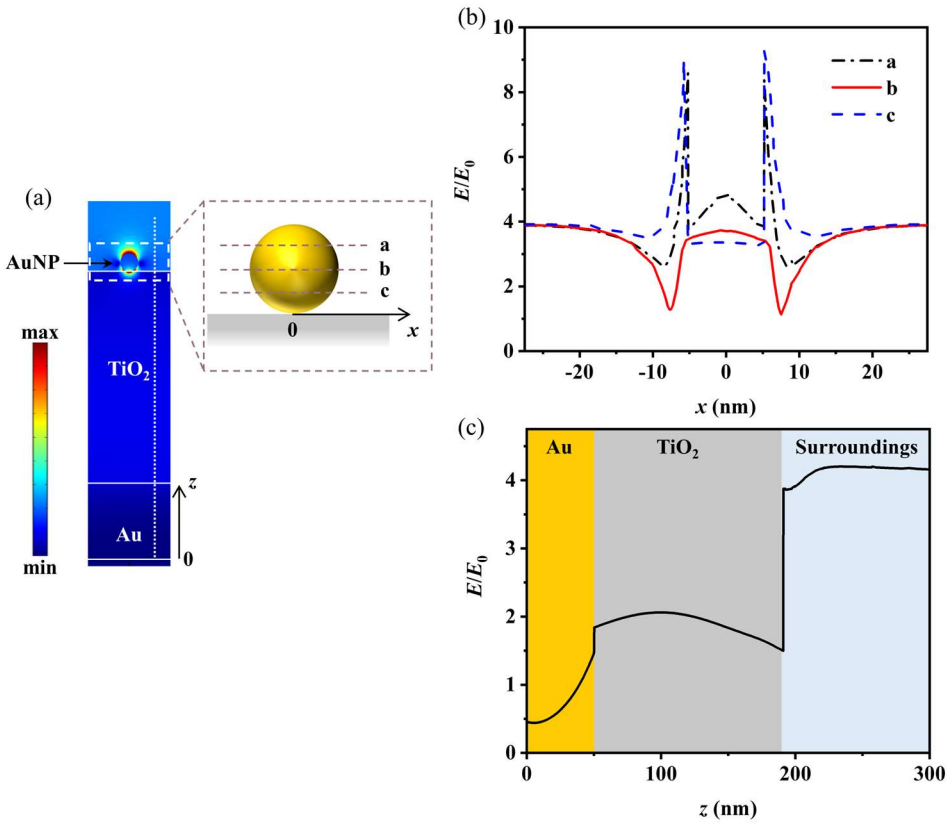


***Fig. S5 (a) Electric field distribution of PWR-LSP at the resonance wavelength when an isolated AuNP is placed on the surface of $TiO_2$. Inset is a simplified enlargement diagram of the local Au-$TiO_2$-AuNPs structure and not drawn to scale. (b) Values of $E/E_0$ along the dashed purple lines in the inset of (a). (c) Values of $E/E_0$ along the dotted white line in (a).***

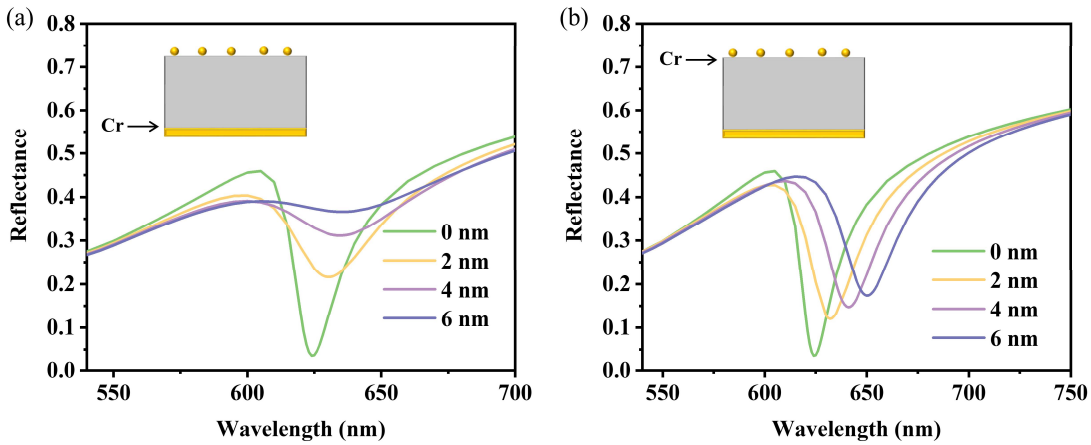


**Fig. S6** (a) Effect of the thickness of the Cr layer between $TiO_2$ and Au layers on reflection spectra of the PWR-LSP sensor. (b) Effect of the thickness of the Cr layer between the $TiO_2$ layer and AuNPs on reflection spectra of the PWR-LSP sensor.

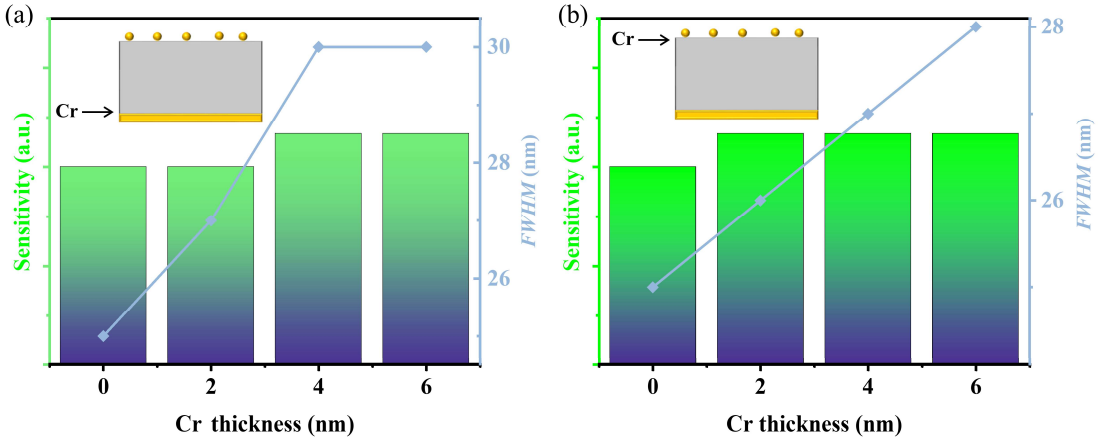


**Fig. S7** (a) Effect of the thickness of the Cr layer between $TiO_2$ and Au layers on the sensitivity and *FWHM* of the PWR-LSP sensor. (b) Effect of the thickness of the Cr layer between the $TiO_2$ layer and AuNPs on the sensitivity and *FWHM* of the PWR-LSP structure.

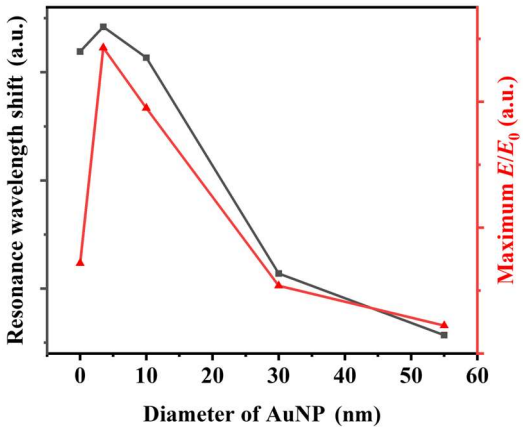


***Fig. S8 Effect of the AuNP diameter on the resonance wavelength shift and maximum $E/E_0$. Resonance wavelength shift corresponds to the difference of resonance wavelengths of reflection spectra with surrounding refractive indices of 1.3323 and 1.3329.***

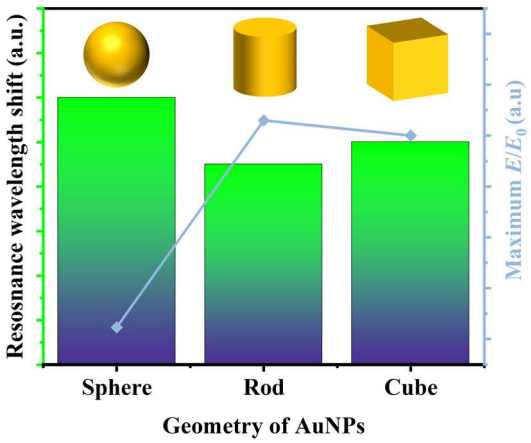


***Fig. S9 Effect of the geometry of AuNPs on the resonance wavelength shift and maximum $E/E_0$. Resonance wavelength shift corresponds to the difference of resonance wavelengths of reflection spectra with surrounding refractive indices of 1.3323 and 1.3329. The diameter of the sphere, the height and diameter of the rod, and the side length of the cube are all 12 nm.***

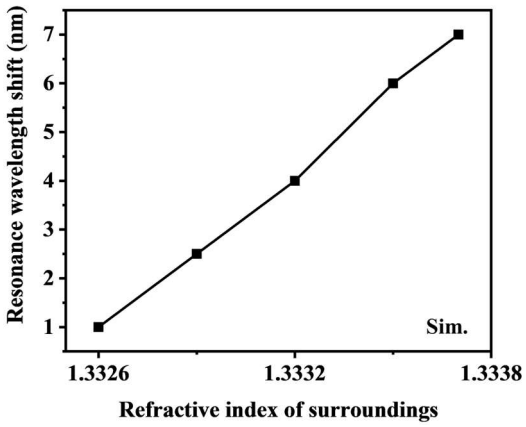


***Fig. S10 Resonance wavelength shift with the increase of the refractive index of surroundings. The resonance wavelength of the reflection spectrum corresponding to a surrounding refractive index of 1.3323 is regarded as the initial resonance wavelength.***

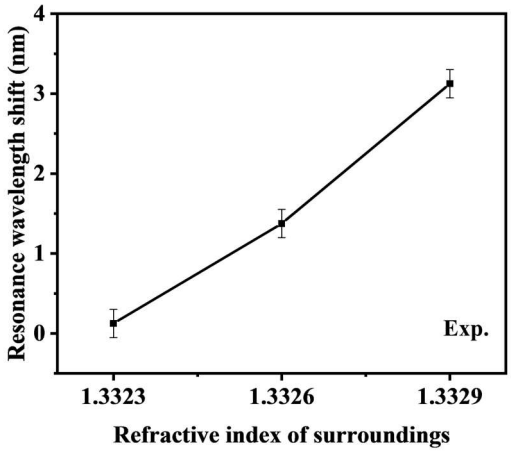


***Fig. S11 Resonance wavelength shift of the PWR-LSP sensor when exposed to the water, 0.25% glycerin solution, and 0.5% glycerin solution. The refractive indices of the water, 0.25% glycerin solution, and 0.5% glycerin solution are 1.3323, 1.3326, and 1.3329 respectively.***

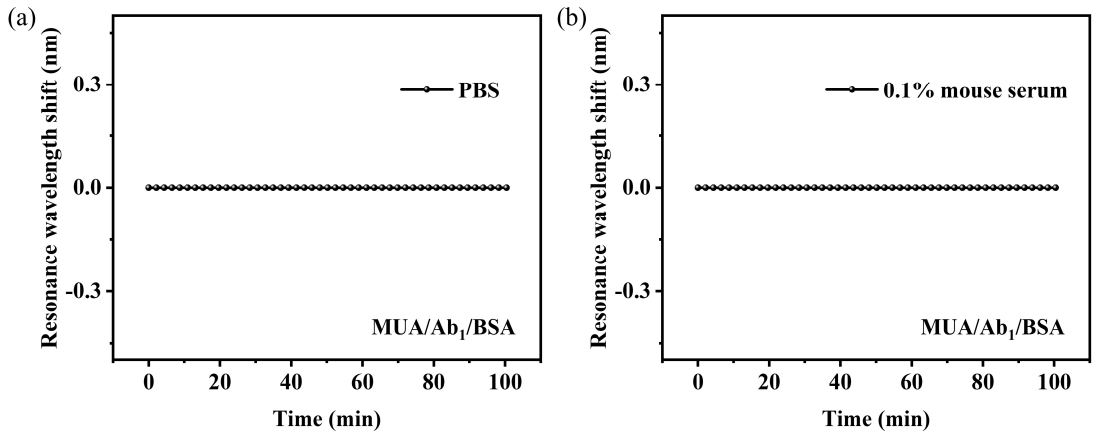


**Fig. S12** Resonance wavelength stability of the PWR-LSP biosensor with the MUA/$Ab_1$/BSA modification in PBS (a) and 0.1% mouse serum (b).

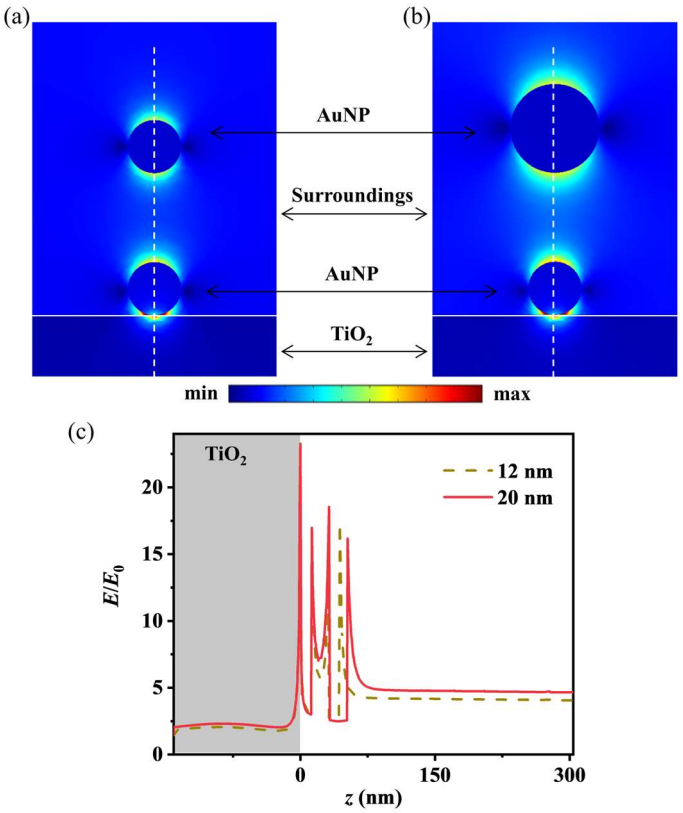


***Fig. S13 Electric field perturbation of the PWR-LSP mode when AuNPs with diameters of 12 nm (a) or 20 nm (b) are placed at 20 nm away from the top of the Au-$TiO_2$-AuNPs. (a) and (b) only exhibit electric field distributions of the AuNPs and their nearby region. (c) Dashed yellow line and solid red line are values of $E/E_0$ along dashed white lines in (a) and (b), respectively.***